Analysis and implementation of peak armature current (Imax) of a chopper-fed DC-DC motor drive in DCM

Mohamad Nazir Abdullah, Muhammad Hafeez Mohamed Hariri, Mohd Khairunaz Mat Desa, Mohd Nadzri Mamat, Suardi Kaharuddin
School of Electrical and Electronic Engineering, Universiti Sains Malaysia (USM), Nibong Tebal, Malaysia

## Article Info

ABSTRACT

At low frequencies of operation in a chopper-fed direct current (DC) motor drive, the armature current may become discontinuous thus the controller operates in discontinuous conduction mode (DCM). Since the minimum armature current is zero in DCM, the analysis of peak armature current (Imax) is to investigate the ripple content in armature current at different values of duty cycle which will help in decreasing the peaky current of DC motor during operation. The simulation was carried out using MATLAB-Simulink software and the laboratory setup was based on Atmega 328 microcontroller board. In this paper, the theoretical and experimental analysis of peak armature current were performed at fix low frequency in DCM and variable duty cycles to provide full control of DC motor speed. The results show that the peak armature current changes with the change of duty cycles and its magnitude is decreased almost 50% at higher duty cycle values.
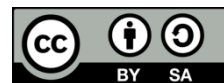
Corresponding Author:

Muhammad Hafeez Mohamed Hariri
School of Electrical and Electronic Engineering, Universiti Sains Malaysia (USM)
Nibong Tebal, 14300, Penang, Malaysia
Email: muhammadhafeez@usm.my

1. INTRODUCTION

Direct current (DC) motor drives can be categorized into two main topologies depending on the type of input source. The topologies are phase controlled DC motor drive and chopper-fed DC motor drive as shown in Figure 1. In phase controlled either AC motor or DC motor drives, the input supply is alternating current (AC) single or three phase sources [1]. The controller is a bridge thyristor-based rectifier AC to DC converter which converts the AC input into a controllable variable output DC as illustrated in Figure 1(a). The speed control is obtained by controlling the firing angle of the thyristor that varies the mean value of the rectified voltage [2], [3]. The disadvantages of using this topology is it produces high ripple in the output voltage and high pulsating armature current and lead to the heating of DC motor [3]. Another point is poor power factor on the AC side in phase control need to be taken into consideration while using this topology.

In chopper-fed DC-DC motor drive shown in Figure 1(b), the power conversion is only working in DC when the input supply is DC power source or batteries. The speed control is obtained by controlling the duty cycle triggered to the gate of the switch at certain switching frequency and the variable converter's output voltage is obtained [3]-[5]. This topology provides significant advantages like low output voltage ripple, low pulsating armature current and great efficiency [6]. The armature current of circuit presented in Figure 1(b) can be analyzed based on continuous conduction mode (CCM) and discontinuous conduction mode (DCM) modes [7]. There are several factors which may lead the converter to operate in CCM or DCM. The operation of the converter in a chopper-fed DC motor drive is in CCM or DCM depends on the motor resistance R_a, motor inductance L_a, duty cycle k and chopper's switching frequency, f_s.
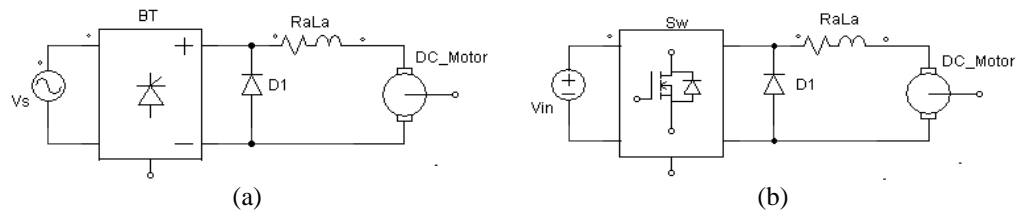
Figure 1. AC-DC motor drive system: (a) phase-controlled DC motor drive and
(b) chopper-fed DC motor drive

In many applications, CCM is employed. When designing a converter with a priority given to reduce the output ripple voltage, CCM is used. In CCM, the value of the armature current of the converter is always positive and varies between minimum and maximum values. Unlike in CCM, the value of the armature current changes between zero level and a positive value in DCM at a certain period of time. At light load (small motor current), operating the converter at high frequency in CCM may increase the switching losses of MOSFET thus reducing the efficiency of the converter. This is a common drawback to chopper-fed DC motor drive systems. In order to improve the efficiency of light load applications, DCM is generally applied. However, the peak armature current is the main issue since it becomes large in DCM mode. If we consider the switching frequency of the chopper is low frequency and the armature inductance of the DC motor, L_a is too small, the armature current will be operating in DCM [8]. The DCM mode usually occurs in converters which consist of the single-quadrant switch with a freewheeling diode and may also occur in converters with two-quadrant switches. In converters of the single-quadrant switch with another switch to replace the freewheeling diode like in a synchronous rectifier, the converter efficiency may be increased and DCM mode can be avoided. Many converters are developed for applications in DC motor drives in order to improve higher efficiency and smaller size or volume, where high switching frequencies can be applied to the converters [9], [10].

The LLC-LC resonant converter fed permanent magnet direct current or PMDC motor which was proposed in [11] was more efficient with a smaller gap switching frequency range for a wide range of load variation applications. Similarly, a paper in [12] suggested a three-phase series-parallel resonant converter-fed DC-dive system that has zero switching losses at higher switching frequencies. The research done by [13] uses four-quadrant zero current transition (ZCT) converter-fed DC motor drives for electric propulsion which has advantages in reducing switching stress at zero current switching. Modeling and simulation of AC-DC buck-boost converter fed DC motor with uniform pulse width modulation (PWM) technique was implemented in [14] to suit as a front-end power source in variable speed drive system. Many papers in the literature review have discussed their study in CCM and DCM. In [15], a characterized control of a four-quadrant DC-DC converter operating CCM and DCM was developed to limit the input current. A new modeling method based on proportional calculus and linear constraints for Boost converter in CCM and DCM was proposed in [16] while the paper in [17] has presented and validated the comparison of efficiencies of junction field effect transistor (JFET) and insulated-gate bipolar transistor IGBT for full bridge converter operated under CCM and DCM. A power loss analysis of active clamp forward converter in CCM and DCM was presented in [18] to increase the efficiency of light load applications. In terms of speed control, there are several papers have presented their study. A separate DC motor speed controller based on four-quadrant choppers was presented in [19]. This includes a four-quadrant operation of a DC motor with a digital control strategy which was proposed in [20] while the paper in [21] investigated a comparative and robustness analysis of closed-loop speed control for four-quadrant choppers. A detailed analysis on DC choppers and speed control techniques was performed in [22] to study their performance.

This paper also examines the armature current of a chopper-fed DC motor in CCM and DCM modes. In section 2, the first quadrant DC chopper design is proposed and the mathematical model is presented. The specific analysis on the armature current of the converter in CCM and DCM is also presented. In section 3, the calculation and simulation of the peak armature current of the converter in DCM are shown. The experimental prototype and verified results are described in section 4. The paper is concluded in section 5.

2. CHOPPER-FED DC MOTOR DRIVE

A DC chopper or commonly known as a DC-DC converter is a driver that changes fix DC input voltage to a certain value of DC output voltage. A chopper-fed DC motor drive uses a power electronic switch, typically a thyristor or transistor, to regulate the voltage supplied to a DC motor by rapidly turning the supply on and off. DC motor is widely used in adjustable speed drive and position control of applications like rapid transit systems, robotic drives, pedal-assisted bicycles, trolley cars, and traction motor control [23]-[25].

2.1. Buck DC chopper design

A first quadrant chopper-fed DC motor drive based on a buck converter is drawn in Figure 2. In this circuit, the DC motor is equivalent to the combination of an internal resistance R_a, an internal inductance L_a in series with back EMF voltage E [26]. The buck converter comprises a fast recovery diode D_1 and an active switch $SW1$ in series with a DC input supply V_D.

The DC input supply is applied to the DC motor when the switch is ON. The current is conducted from the source to the internal winding of the DC motor. In the first quadrant DC chopper, the motor (armature) current I_a of the DC motor is in one direction and the polarity of the terminal output voltage or known as motor (armature) voltage V_a cannot be reversed. When the chopper is OFF, the DC input supply is disconnected from the DC motor. The energy is stored in the internal inductance and the back EMF of the motor drives the internal current through a fast recovery diode. This condition is valid for CCM only. Both the internal current and the motor voltage will be always positive. The motor voltage however can be controlled from zero to the maximum rated voltage by altering the duty cycle of the switch. This makes a DC motor controllable over a wide range of speeds.

2.2. Modelling of DC chopper

Generally, a model of a DC chopper can be developed using the operation modes and current conduction modes of the converter. There are three operation modes have been considered for the converter over a full switching cycle and these modes are illustrated in Figures 3(a)-3(c). The state variables will describe the dynamic behavior of a chopper-fed DC motor based on the switching states of $SW1$ and the diode $D1$. Considering the waveform characteristic of armature current conducted through the DC motor, the model will be derived based on the current conduction modes of the converter in CCM and DCM. The gate switching voltage for switch V_g, the motor voltage $V_{a,}$ and the motor current I_a waveforms of chopper-fed DC motor in CCM and DCM are shown in Figures 4(a) and 4(b), where I_{max} and I_{min} are the maximum values and minimum value of the motor current respectively.
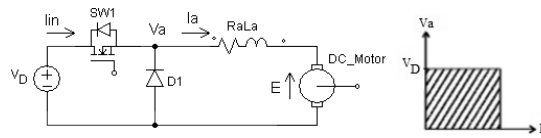

Figure 2. Buck converter DC motor drive with first quadrant operation
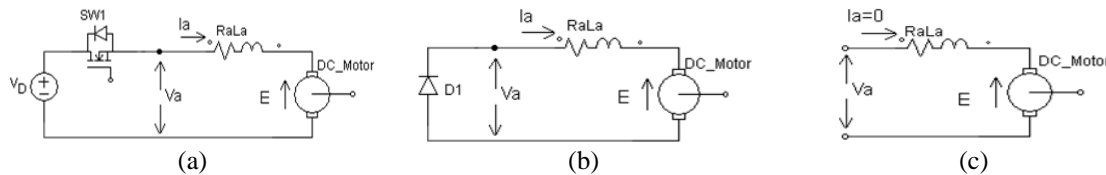

(a)   (b)   (c)

Figure 3. Operating modes of chopper-fed DC motor: (a) Mode 1: SW1 ON, D1 OFF,
(b) Mode 2: SW1 OFF, D1 ON, and (c) Mode 3: SW1 OFF, D1 OFF

(a)   (b)

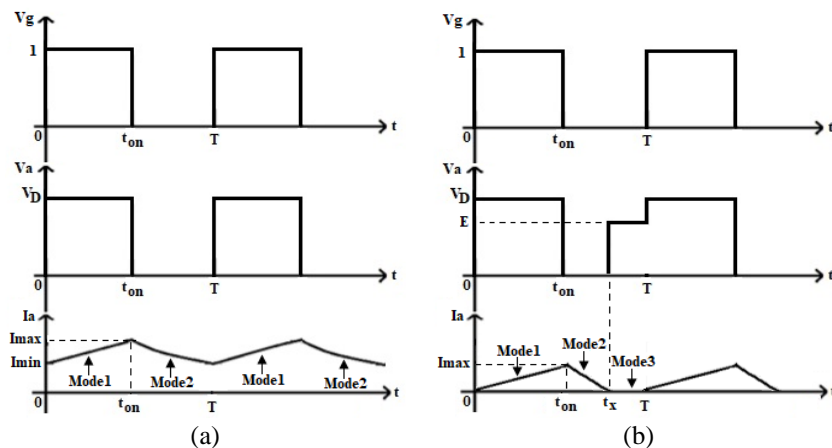Figure 4. Switching state, armature voltage, and armature current: (a) CCM and (b) DCM

3.   SIMULATION OF PEAK DCM ARMATURE CURRENT

In order to analyze the value of peak armature current, a powerful simulation tool software is required. The simulation setup is carried out using the MATLAB/Simulink software. MATLAB/Simulink was chosen because it has powerful and modern features.

3.1. Simulation results

Through Simulink, the circuit design can be created, and the desired output waveforms can be viewed clearly. In addition, a real-time simulation offered in MATLAB/Simulink is used to predict and characterize the behavior of inputs and outputs in an actual hardware implementation. The simulation circuit model for the chopper-fed DC motor drive is shown in Figure 5. The converter consists of input supply V_D, buck subsystem, and output parameters. The subsystem consists of a buck converter and DC motor model. The gating signal V_g is the pulse generated by the duty cycle d and the PWM generator block. The simulation was performed at fixed input voltage and fixed switching frequency. In the simulation, the circuit was assumed to operate in ideal circuit parameters. The simulation was also conducted in no load condition without any load attached to the motor (TL = 0). There is no feedback controller required since the chopper-fed DC motor was operating in the first quadrant, and its speed was determined directly by the duty cycle.
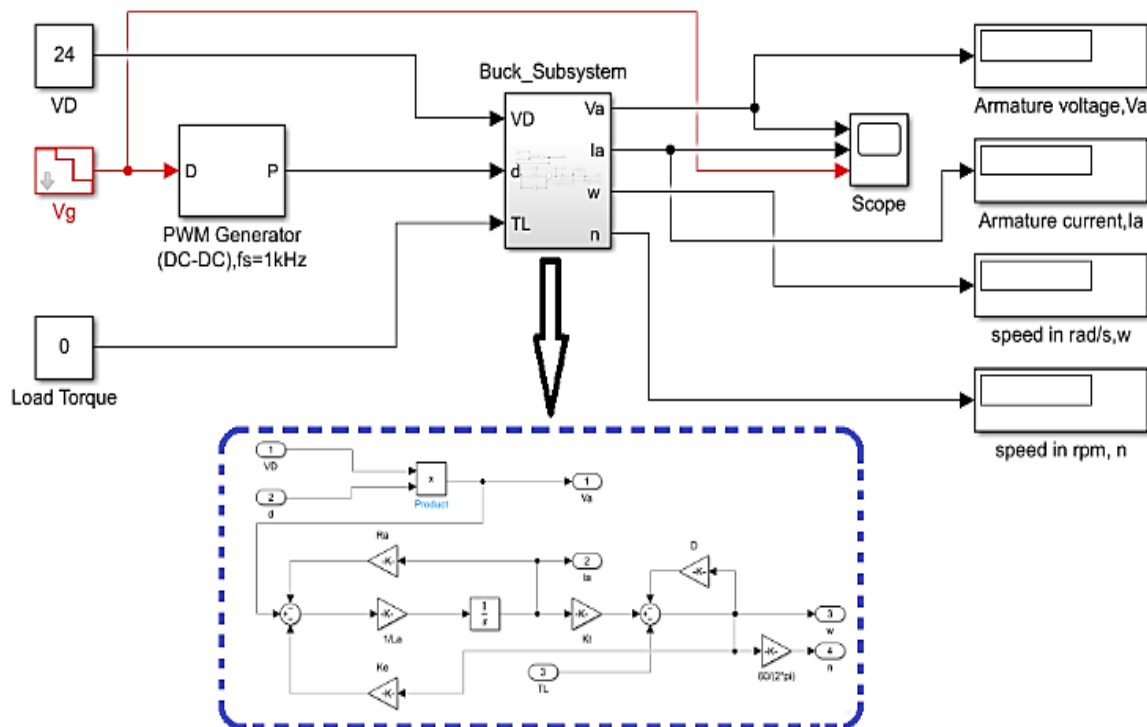

Figure 5. Simulation circuit model in MATLAB/Simulink

The input voltage was set to 24 V and the PWM gating signal were varied from minimum 0 to maximum 1. The simulation results for no-load condition are displayed in the following figures. The switching frequency was fixed at 1kHz. The motor voltage, the input current and the motor current waveforms for the simulation circuit are displayed in Figure 6(a) and Figure 6(b) at k = 0.2 and k = 0.4 respectively.

In the above two plots, the motor armature current waveforms show that the chopper-fed DC motor operates in DCM. At the beginning of SW1 ON, the armature current rises up slowly from zero to peak value until it is OFF. The armature current continues to flow in a short time but abruptly drops to zero due to small value of armature inductance existed in DC motor. At the remaining period of time, during the switch is turned OFF, it returns to zero indicating that the converter is running in DCM. In Figures 6(a) and 6(b), by using the peak finder feature in MATLAB/Simulink, the peak armature current waveforms were recorded at 7.60 A when $k = 0.2$ and at 6.40 A when $k = 0.4$. The waveforms are shown in the intervals between 11.4765 s to 11.7295 s as the outputs were in a steady state condition during this period.
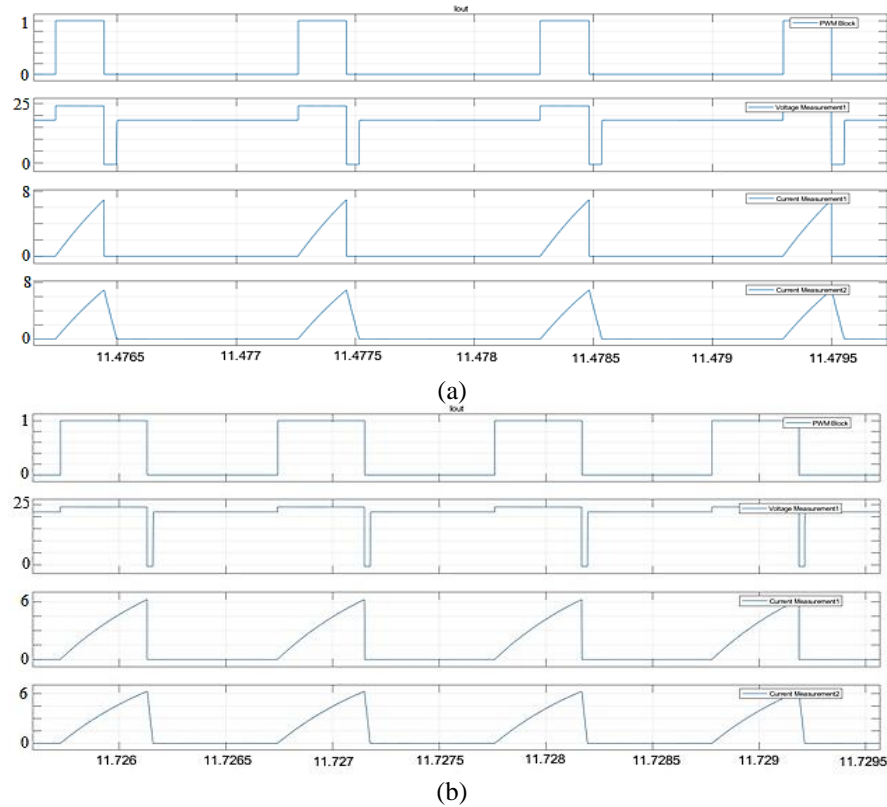
(a)

(b)

Figure 6. Waveforms for chopper-fed DC motor in DCM mode. From top to bottom: V_g, V_a, I_{in} and I_a:
(a) $k = 0.2$ and (b) $k = 0.4$

4. EXPERIMENTAL VALIDATION

Experimental validation involves conducting hardware circuitry tests to verify the performance and accuracy of a proposed prototype. The measured data based on the experimental setup are compared with the expected results to validate its reliability and performance. In practice, the actual switch is realized by using a power MOSFET which can be operated at a high current in several amperes.

4.1. Experimental setup

The circuit realization of Figure 5 employs a single quadrant switch. The switch only allows the power to flow in one direction, which is from the DC source to the load. Figure 7 shows the experimental setup of chopper-fed DC motor drive system. Experimental work was performed in a laboratory workbench to validate the previous simulation results.
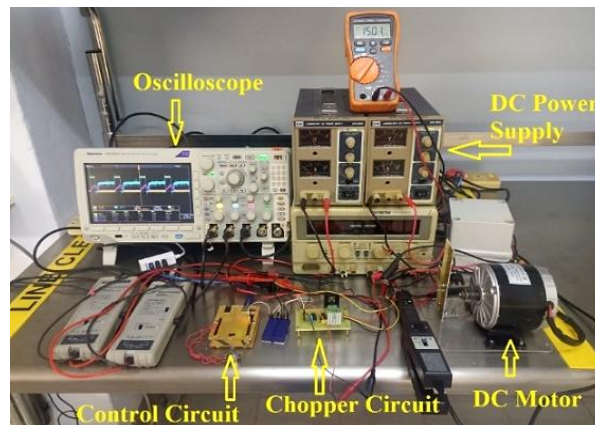

Figure 7. The experimental setup

The parameters of prototype are the same as used in the simulation section. The prototype is composed of chopper power stage circuit, PWM control circuit, DC motor, DC power supply and signal conditioning equipment. Two regulated DC power supplies were used, one supplying the chopper circuit and another one for PWM control circuit. The first DC power supply output was set at 12 V for PWM control circuit and the other power supply output at 24 V to the chopper circuit. The chopper circuit was built based on a high power and high speed MOSFET IRFZ44N combined with a high speed Schottky diode MUR860. The chopper setup was then fed with a DC motor. The voltage measurement was done using the Agilent N2791A differential probe while the input and the armature current measurements were done using the Tektronix A622 AC/DC current probe. All these measurements were then displayed on the Tektronix MD03024, a 4-channel digital oscilloscope. The speed of DC motor was obtained by reading and converting the frequency of pulse generated by an optical encoder Sunx PMT53B which is mounted on the shaft of the motor.

4.2. PWM control methodology

As we know, if the converter operates in DCM, the peak armature current can be controlled from zero to its maximum value. By taking consideration the variation of E, a control system can be designed to vary the duty cycle and produce the peak armature current at a certain value. The control system was developed so that the DC motor speed linearly changed when the duty cycle is adjusted. Since the DC motor was not attached to any load, the value of E will also change linearly. The method of control used is a pulse width modulation (PWM) and constant low frequency control as shown in Figure 8.

The implementation of the control circuit was divided into two parts. The first part is using the Atmega 328 microcontroller board to generate a periodic PWM signal, which was used as a gating signal to drive the power MOSFET by turning it ON and OFF alternately. The microcontroller board PWM pin was then connected to one of the differential probes so that the duty cycle and the frequency of PWM signal can be monitored using digital oscilloscope. The control circuit period was set to 1 ms, therefore the lower switching frequency can be obtained at 1 kHz. The second part of the control circuit consists of two integrated chip used as the drive circuit for the power MOSFET. The PWM signal for the switch which was generated by microcontroller was only at 5 V amplitude. It is required to level up the PWM signal to 12 V amplitude in order to charge and discharge the capacitance in MOSFET. The first MOSFET driver chip TC4427 did this job. Since chopper-fed DC motor converter has a MOSFET floating in the circuit, the second chip IR2101 was needed to provide floating reference for the MOSFET as shown in Figure 9. Only then the control PWM output signal can be fed into the switch through the driver circuits.
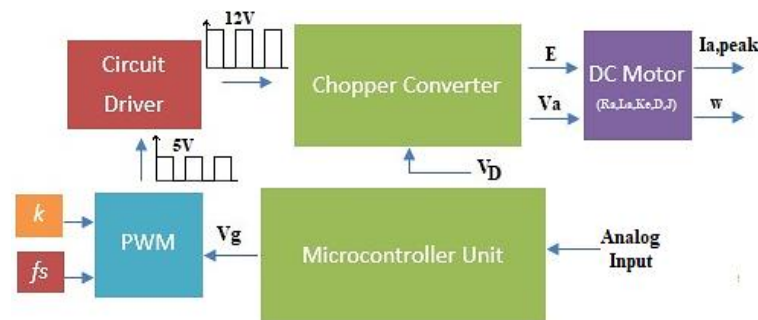

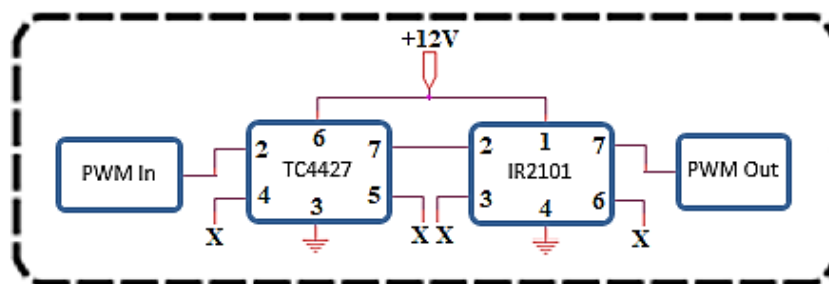Figure 8. Block diagram of constant low frequency control

Figure 9. MOSFET driver circuit

4.3. Experimental results

Table 1 lists the obtained experimental results of the converter at steady state condition. The results are based on measurements done using Agilent U1232A digital multimeters for rms motor voltage and rms motor current. The motor speed in rpm is determined by multiplying the recorded frequency of the encoder output signal with 60. The back EMF voltage is calculated by multiplying the motor speed with the back EMF constant. The peak armature current is recorded from peak-to-peak waveform displayed in the oscilloscope. By adjusting the duty cycle, a wide range of motor voltage, motor current and motor speed can be obtained. It is clearly shown that the motor voltage can be controlled from 0 to 22.10 V when duty cycle is varied between $k = 0$ to $k = 1.0$. The rms motor current varied from 0 to 1.20 A and the calculated motor speed were 0 to 3150 rpm experimentally.

The obtained results of the armature voltage, the total input current and the motor armature current of converter at different duty cycles operating in DCM are shown in Figure 10. In DCM, regardless of value of k, the minimum armature current is zero. The ultrafast diode has prevented the armature current from going to negative value. The recorded peak or maximum value occurred at $t=t_{on}$ during mode 1. The armature current decreased to zero again at $t=t_x$ during mode 2. At this point the armature voltage equals to the value of back EMF voltage as can be seen as flat line at lower duty cycles. Although the rms armature current $I_{a,rms}$ does not show any significant increase when k is increased, we can see that the peak armature current $I_{max,DCM}$ is extremely high at low duty cycles. The peak armature current magnitude is almost 6 to 7 times higher than the rms armature current. The peak armature currents show some declining pattern when k is increased but the magnitudes are still almost 4 to 5 times higher. As k increased, the peak armature current magnitude tends to be reduced to 4.0 A while its maximum value is at 7.80 A. This reduction results in the armature current to behave more stable and regulated while conducting in DCM.

Table 1. Peak motor armature current measurements in DCM

k	V_a, (V)	$I_{a,rms}$, (A)	n,(rpm)	E, (V)	$I_{max,DCM}$, (A)
0	0	0	0	0	0
0.1	6.00	0.74	573	4.00	7.80
0.2	11.95	0.96	1596	11.15	7.79
0.4	17.90	1.10	2484	17..35	6.20
0.6	20.20	1.16	2862	19.99	5.22
0.8	21.34	1.17	3021	21.10	4.59
0.98	21.70	1.19	3078	21.50	4.49
1	22.10	1.20	3150	22.00	4.00

The measured waveforms of armature voltages and peak armature currents as depicted in the above figure has clearly shown that the converter operated in three modes as discussed in section 2.2. Practically, the interval time of mode 2 is very short and it depends on the value of k. At $k = 1$, the interval was 200 us while at $k = 0.98$ the interval was 40 us. This implies the time taken for armature current to become zero. Comparing results obtained in Table 1 with Figures 10(a) and 10(b), it comes to conclusion that the peak values of the armature current in the experimental results and the simulation results are very close to each other for duty cycle above 0.2. At $k = 0.1$, there is small different because the back EMF voltage differs around 2 V between simulation and experiment. Therefore, overall experiment results are consistent with the simulation part, which confirm the validity of the analysis presented in this paper. The simulated and experimental results of peak armature currents versus the duty cycle are represented by the curves shown in Figure 11. If we do the comparison between these two curves, we can see that the waveforms pattern of the peak armature current between experiment and simulation are almost the same each other. The pattern shows an almost nonlinear characteristic for these two waveforms.

At higher duty cycles, from the experimental results waveforms, the back EMF voltage seems not so stable and keep changing as we can see in Figures 10(c)-10(f). Therefore, the readings taken for back EMF voltage is averaged over the whole period of time. The design of chopper-fed DC motor drive system is really applicable for low and light load power applications, such as low frequency power supplies and low power motor drives. For starting the DC motors at lower starting peak armature current, this system will do its job perfectly. In summary, the first quadrant chopper converter can be more effective when using a DC motor in any electric drive system. The main thing to be considered by designers is the peak armature current which appears to be quite high compared to the rms value. Figure 11 also shows the ripple content of armature current of the motor can be made lower by operating the converter at high duty cycles. The difference between simulated and experimental result are caused by the switching device losses and the nonlinearity characteristic of back EMF voltage. In the calculation, losses are negligible during the analysis since all the components are assumed to be ideal.
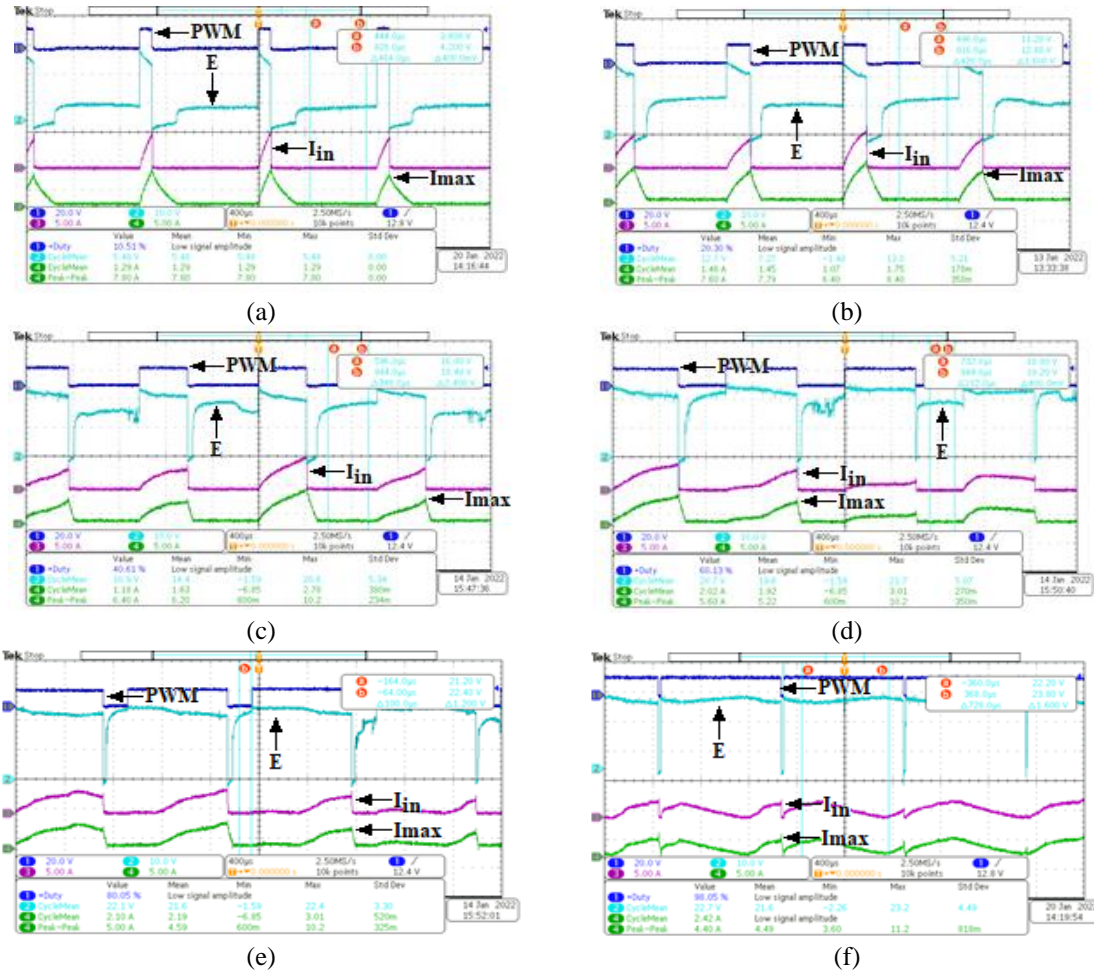
Figure 10. Experimental waveforms at different duty cycles. From top to bottom: V_g (blue), V_a (cyan), I_{in} (purple) and I_a (green): (a) $k = 0.1$, (b) $k = 0.2$, (c) $k = 0.4$, (d) $k = 0.6$, (e) $k = 0.8$, and (f) $k = 0.98$
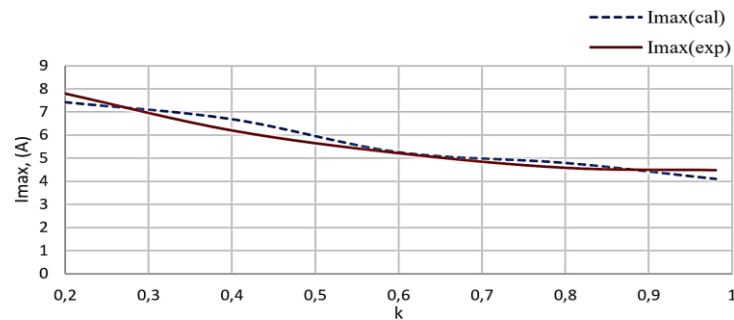

Figure 11. Comparison between the simulated (cal) and measured (exp) of peak armature current (I_{max}) in DCM at different duty cycles

5. CONCLUSION

In this paper, the analysis of peak armature current for the implementation of a chopper-fed DC motor drive system has been discussed in detail. The main focus in this paper is about to monitor the maximum armature current values that is produced at different duty cycles when the converter operating in DCM at light load. The model only used a single quadrant buck converter with a DC motor attached together. The peak armature current of this drive system is presented in computer simulation. The laboratory tests were tested at fix frequency in order to compare the peak armature current magnitude at variable duty cycles. The results show that the peak armature current changes with the change of duty cycles and the peak armature current

magnitude is decreased almost 50% at higher duty cycle values. Due to high peak armature current, the chopper-fed DC motor is more suitable for any electrical drive system running at low power applications.

ACKNOWLEDGEMENTS

REFERENCES

[1] P. Xu, J. Xiao, and Y. Dan, "Multi-rate input based model predictive control for permanent magnet synchronous motor," *Journal of Electrical Systems*, vol. 14, no. 1, pp. 130–142, 2018.

[2] D. A. Barkas, G. C. Ioannidis, C. S. Psomopoulos, S. D. Kaminaris, and G. A. Vokas, "Brushed DC motor drives for industrial and automobile applications with emphasis on control techniques: a comprehensive review," *Electronics*, vol. 9, no. 6, p. 887, May 2020, doi: 10.3390/electronics9060887.

[3] G. C. Ioannidis *et al.*, "AC-DC & DC-DC converters for DC motor drives," in *Proceedings of the 2013 International Conference on Electronics and Communication Systems*, 2013, pp. 96–103.

[4] A. Al-Mayyahi and A. Obed, "Effect of duty cycle and chopper frequency of PWM DC-DC converter drive on performance characteristics of DC motor," in *Conference: The 4th International Scientific Conference of Salahaddin University-Erbil*, 2011.

[5] S. N. Al-Bargothi, G. M. Qaryouti, and Q. M. Jaber, "Speed control of DC motor using conventional and adaptive PID controllers," *Indonesian Journal of Electrical Engineering and Computer Science*, vol. 16, no. 3, pp. 1221–1228, Dec. 2019, doi: 10.11591/ijeecs.v16.i3.pp1221-1228.

[6] A. Raikwar, C. S. Sharma, and M. E. Scholar, "Chopper fed closed loop speed controller system for separately exited DC motor for industrial application using PI controller," *Engineering*, 2021.

[7] B. A. Nasir, Az. M. Abdullah, and O. M. Ali, "Continuous and discontinuous operation of D.C motor fed from thyristor chopper," *Al-Taqani*, vol. 26, no. 2, pp. 9–27, 2013.

[8] B. Eskandari, H. V. Haghi, M. T. Bina, and M. A. Golkar, "An experimental prototype of buck converter fed series DC motor implementing speed and current controls," in *2010 International Conference on Computer Applications and Industrial Electronics*, IEEE, Dec. 2010, pp. 606–609. doi: 10.1109/ICCAIE.2010.5735006.

[9] I. I. Abdalla, E. Zainal, A. R. T. Anwarudin, F. Firmansyah, A. R. A. Aziz, and M. Heikal, "Cogging force issues of permanent magnet linear generator for electric vehicle," *Journal of Electrical Systems*, vol. 13, no. 3, pp. 489–502, 2017.

[10] I. Yahia, C. Ben Salah, and M. F. Mimouni, "Optimal contribution of energy management of electric vehicles," *Journal Electrical Systems*, vol. 12, no. 4, pp. 660–671, 2016.

[11] M. S. Rani and S. S. Dash, "Peformance analysis of LLC-LC resonant converter fed PMDC motor," *International Journal of Control and Automation*, vol. 8, no. 4, pp. 117–136, Apr. 2015, doi: 10.14257/ijca.2015.8.4.14.

[12] M. Daigavane, H. Suryawanshi, and J. Khan, "A novel three phase series-parallel resonant converter fed DC-drive system," *The Korean Institute of Power Electronics Journal of Power Electronics*, vol. 7, no. 3, pp. 222–232, 2007.

[13] T. W. Ching, "Four-quadrant zero-current-transition converter-fed DC motor drives for electric propulsion," *Journal of Asian Electric Vehicles*, pp. 911–917, 2005, doi: 10.4130/JAEV.3.651.

[14] N. A. Ahmed, "Modeling and simulation of ac–dc buck-boost converter fed dc motor with uniform PWM technique," *Electric Power Systems Research*, vol. 73, no. 3, pp. 363–372, Mar. 2005, doi: 10.1016/j.epsr.2004.08.010.

[15] H. Chaoui, M. Alzayed, O. Okoye, and M. Khayamy, "Adaptive control of four-quadrant DC-DC converters in both discontinuous and continuous conduction modes," *Energies*, vol. 13, no. 16, p. 4187, Aug. 2020, doi: 10.3390/en13164187.

[16] J. Han, B. Zhang, and D. Qiu, "Unified model of boost converter in continuous and discontinuous conduction modes," *IET Power Electronics*, vol. 9, no. 10, pp. 2036–2043, Aug. 2016, doi: 10.1049/iet-pel.2015.0754.

[17] V. V. S. K. Bhajana, P. Drabek, M. Jara, and Z. Peroutka, "Comparison of main design concepts of auxiliary drives for DC catenary fed light traction vehicles: SiC JFET vs Si IGBT technology," *EPE Journal*, vol. 31, no. 1, pp. 17–31, Jan. 2021, doi: 10.1080/09398368.2020.1811573.

[18] S. Xu, T. Zhang, Y. Yao, and W. Sun, "Power loss analysis of active clamp forward converter in continuous conduction mode and discontinuous conduction mode operating modes," *IET Power Electronics*, vol. 6, no. 6, pp. 1142–1150, Jul. 2013, doi: 10.1049/iet-pel.2013.0019.

[19] A. I. Umeogamba, C. U. Ogbuka, and E. Ejiogu, "Armature voltage speed control of a separately excited DC motor using four quadrant chopper," *IEEE 1st International Conference on Mechatronics, Automation and Cyber-Physical Computer System*, pp. 29–35, 2019.

[20] P. B, P. K. S. Chinamalli, and R. Yanamshetti, "Digital control strategy for four quadrant operation of DC motor using DSPIC30F4011," *International Journal of Recent Technology and Engineering (IJRTE)*, vol. 3, no. 3, pp. 73–77, 2014.

[21] C. K. Das and S. K. Swain, "Closed loop speed control of chopper fed DC motor for industrial drive application," in *2017 International Conference on Power and Embedded Drive Control (ICPEDC)*, IEEE, Mar. 2017, pp. 478–483. doi: 10.1109/ICPEDC.2017.8081137.

[22] M. R. Çorapsiz, B. Alim, and H. Kahveci, "Detailed analysis of DC choppers and an example of PMDC motor speed control," *Eastern Anatolian Journal of Science*, vol. IV, no. I, pp. 16–36, 2018.

[23] F. E. Hoyos Velasco, J. E. Candelo-Becerra, and A. Rincón Santamaría, "Dynamic analysis of a permanent magnet DC motor using a buck converter controlled by ZAD-FPIC," *Energies*, vol. 11, no. 12, p. 3388, Dec. 2018, doi: 10.3390/en11123388.

[24] E. Hernández-Márquez *et al.*, "Robust tracking controller for a DC/DC buck-boost converter–inverter–DC motor system," *Energies*, vol. 11, no. 10, p. 2500, Sep. 2018, doi: 10.3390/en11102500.

[25] M. Rodič, M. Milanovič, and M. Truntič, "Digital control of an interleaving operated buck-boost synchronous converter used in a low-cost testing system for an automotive powertrain," *Energies*, vol. 11, no. 9, p. 2290, Aug. 2018, doi: 10.3390/en11092290.

[26] M. N. Abdullah, M. K. Mat Desa, E. A. Bakar, and M. N. Akhtar, "Experimental and numerical studies for parameters identification of direct current motor," *Indonesian Journal of Electrical Engineering and Computer Science*, vol. 27, no. 2, pp. 592–600, Aug. 2022, doi: 10.11591/ijeecs.v27.i2.pp592-600.

BIOGRAPHIES OF AUTHORS

Mohamad Nazir Abdullah received his B.Eng. in Electrical from Universiti Sains Malaysia (USM) in 2000 and received master of electrical engineering from School of Electric and Electronic Engineering USM in 2009. He joined Universiti Sains Malaysia (USM) as research officer at Electrical Department since 2001. His research interests include power electronics, energy conversion, and renewable energy system. He can be contacted at email: eemnazir@usm.my.

Muhammad Hafeez Mohamed Hariri received a B.Eng. and M.Sc. from the Universiti Sains Malaysia (USM) in 2010 and 2014 respectively. In March 2022, he was awarded his Ph.D. degree from School of Electrical and Electronic Engineering, Universiti Sains Malaysia (USM). He is a registered professional engineer under Board of Engineers Malaysia (BEM) in the electrical track. Currently, he is a senior lecturer at School of Electrical and Electronic Engineering, Universiti Sains Malaysia (USM). He has authored and co-authored number of well recognized journals and conference papers. His research interests are in electrical power systems, power electronics, and renewable energy systems (photovoltaic). He can be contacted at email: muhammadhafeez@usm.my.

Mohd Khairunaz Mat Desa is a member of IEEE. He received the master's degree in Electrical Engineering from Loughborough University, United Kingdom, in 2008 and Ph.D. degree in Renewable Energy from National University of Malaysia, Bangi, Selangor, in 2014. He is a senior lecturer with the School of Electrical and Electronic Engineering, Universiti Sains Malaysia, Nibong Tebal, Malaysia. He is specialized in solar photovoltaics (silicon technology applications), photovoltaic-thermal, renewable energy (wind, biomass, and hydropower), power electronics, and energy policy. He can be contacted at email: khairunaz@usm.my.

Mohd Nadzri Mamat received his B.Eng. in Electrical from Universiti Sains Malaysia (USM) in 2000 and received master of electrical engineering from School of Electric and Electronic Engineering USM in 2009. He joined Universiti Sains Malaysia (USM) as research officer at Electrical Department since 2001. His research interests include electrical power systems, machines, and drives. He can be contacted at email: eenadzri@usm.my.

Suardi Kaharuddin received his B.Eng. in Electrical & Mechatronics from Universiti Sains Malaysia (USM) in 2002 and received master of electrical engineering from School of Electric and Electronic Engineering USM in 2009. He joined Universiti Sains Malaysia (USM) as research officer at Electrical Department since 2002. His research interests include power electronics, microcontroller, and embedded system. He can be contacted at email: suardi@usm.my.